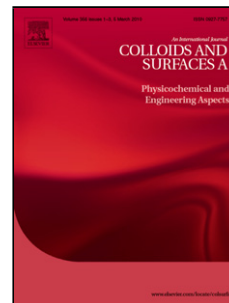


Accepted Manuscript

Title: Hysteresis and Scanning Curves in Linear Arrays of Mesopores with Two Cavities and Three Necks

Author: Yonghong Zeng Shiliang Johnathan Tan D.D. Do D. Nicholson



PII: S0927-7757(15)30166-7
DOI: <http://dx.doi.org/doi:10.1016/j.colsurfa.2015.08.023>
Reference: COLSUA 20114

To appear in: *Colloids and Surfaces A: Physicochem. Eng. Aspects*

Received date: 19-5-2015
Revised date: 6-8-2015
Accepted date: 17-8-2015

Please cite this article as: Yonghong Zeng, Shiliang Johnathan Tan, D.D.Do, D.Nicholson, Hysteresis and Scanning Curves in Linear Arrays of Mesopores with Two Cavities and Three Necks, *Colloids and Surfaces A: Physicochemical and Engineering Aspects* <http://dx.doi.org/10.1016/j.colsurfa.2015.08.023>

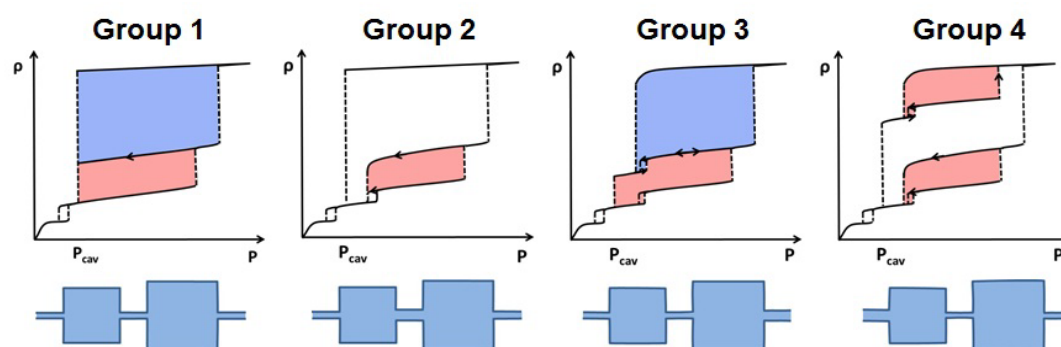
This is a PDF file of an unedited manuscript that has been accepted for publication. As a service to our customers we are providing this early version of the manuscript. The manuscript will undergo copyediting, typesetting, and review of the resulting proof before it is published in its final form. Please note that during the production process errors may be discovered which could affect the content, and all legal disclaimers that apply to the journal pertain.

Hysteresis and Scanning Curves in Linear Arrays of Mesopores with Two Cavities and Three Necks Classification of the Scanning Curves

Yonghong Zeng, Shiliang (Johnathan) Tan, D. D. Do* d.d.do@uq.edu.au, D. Nicholson
School of Chemical Engineering, University of Queensland, St. Lucia, QLD 4072, Australia

*Corresponding author.

Graphical Abstract



Highlights

- A simple model of linear array of mesopores is proposed to study scanning
- Hysteresis and scanning curves are studied in terms of the sizes of the array
- The scanning curves can be classified into four groups
- Scanning curve either span across the hysteresis loop or returns to the same boundary

Abstract

Adsorption of argon at 87K in a linear array of slit mesopores composed of two cavities and three necks has been investigated using Grand Canonical Monte Carlo simulation. Hysteresis and scanning was found to depend on the relative size of the necks and cavities and on whether the necks are wider or narrower than the critical width that demarcates cavitation from pore blocking. There are 26 possible combinations for the linear array. By considering the behaviour of hysteresis scanning curves, we are able to identify four distinct groups:

- (i) Group 1: The descending scanning spans the boundary curve of the hysteresis loop due to stretching of the condensate in the small cavity.
- (ii) Group 2: The descending curve partially spans the loop and returns to the adsorption boundary. This occurs either because the condensate stretches in the small cavity, followed by evaporation via a pore blocking mechanism; or because the condensate evaporates as the meniscus recedes in the large neck that joins the two cavities.
- (iii) Group 3: The descending curve spans the loop as in Group 1 but there is a small sub-loop associated with emptying and filling of the large neck connecting the large cavity to the surrounding gas.
- (iv) Group 4: The descending scanning curve is similar to that in Group 2; but when the large cavity of the array is filled with adsorbate, and the small cavity is empty (except for an adsorbed film) the ascending curve partially spans the loop. This happens when molecular layers build-up in the small cavity (c.f. stretching of condensate in a descending scan) is followed by condensation, which results in the scanning curve returning to the desorption boundary (c.f. evaporation of the condensate and return to the adsorption boundary). There is also a sub-loop which has similar characteristics to those in Group 3.

1 Introduction

In the past few decades, significant progress has been made in understanding adsorption hysteresis, thanks to the synthesis of ordered mesoporous materials, the development of high-resolution apparatus for adsorption measurement, and the availability of increased computing power. The hysteresis loop in an adsorption isotherm is a valuable tool for probing the character of a porous solid, since its size, shape and position are sensitive to adsorbate, temperature and the porous structure¹⁻³. Thus for example, for a given temperature and adsorbate, the boundary loop can be used to derive pore size distribution. Following an earlier analysis by de Boer in 1972⁴, the IUPAC in 1985, classified the shape of experimental hysteresis loops into four types H1 to H4^{5,6}.

Among the various loop shapes, the type H2, which has a gradually increasing adsorption boundary and a steep desorption boundary, is commonly found for disordered solids such as silica gel and Vycor. This loop type has prompted much discussion in the literature about the interconnectivity of pore spaces within an adsorbent. An early attempt to discuss the role of connectivity was put forward by McBain who proposed an “ink-bottle” pore model in which a large cavity is connected to the bulk gas surroundings via necks⁷. It is now well known that desorption from this model pore, when filled with adsorbate, can occur either via pore blocking or by cavitation. In pore blocking, a meniscus (at the interface separating the adsorbed and gas phases) formed at the mouth of the neck, recedes when the pressure is lowered to less than the critical value corresponding to the neck radius, and when it reaches the junction between the neck and the cavity the condensate in the wider cavity instantly evaporates. On the other hand, in the cavitation mechanism, the neck is so small that the condensate in the cavity is stretched until the so-called cavitation pressure for the condensate in the cavity is reached when it becomes mechanically unstable and evaporates, while the neck remains (partially) full⁸⁻¹⁰.

Although the importance of connectivity between cavities via narrower necks has been well recognized, the correlation between connectivity and size distribution in porous solids, and the measured adsorption-desorption isotherm is still not fully understood. A step towards a better appreciation of this correlation is to scan the hysteresis loop by either decreasing pressure from any point on the adsorption boundary (a descending scanning curve) or

increasing pressure from any point on the desorption boundary (an ascending scanning curve) of the boundary hysteresis loop¹¹⁻¹³. This procedure can be further elaborated by reversing the direction of pressure at any point on any scanning curve to give sub-loops. The various terminologies involved in these processes are summarised in Figure 1a. Three types of scanning curve can be identified as follows¹⁴:

- (i) Crossing between the boundary curves of the hysteresis loop.
- (ii) Returning to the same boundary.
- (iii) Intermediate between (i) and (ii), in which the descending and ascending scanning curves converge to the lower and upper closure points, respectively.

These scanning curves are observed when some parts of the adsorbent are filled with adsorbate (Region I), while the other regions (Region II) are still empty, except for molecular layers on the pore walls. The descending scanning curve is associated with stretching of the condensate in Region I, followed by evaporation, and the ascending scanning curve is associated with further layering of molecules on the pore walls in Region II, followed by condensation¹⁵⁻¹⁷.

Recognizing the potential gain of a deeper insight into pore structure, and the growing power of modern adsorption equipment, scanning has been receiving increasing attention in both experimental and theoretical studies¹⁸⁻²⁰. One of the earliest attempts to model the scanning process was the Independent Domain theory proposed by Everett²¹. This theory assumes that a porous solid is an assembly of pores that are filled and emptied independently. Broekhoff *et al.*²² later showed that the experimental scanning is inconsistent with the Everett's theory when more than 50% of the porous network is filled with adsorbate, indicating that the domains are no longer independent; a more recent simulation study by Coasne *et al.*²³ showed that the original theory must be modified to account for the presence of adsorbed layers. Mason²⁴ explored percolation in different pore network models to better understand the effects of connectivity and pore size correlations on scanning. More recent studies include the work of Rojas *et al.*²⁵ who constructed a dual site-bond model for heterogeneous 3D mesoporous networks and Cimino *et al.*²⁶ who formulated a model based on a 3D cubic lattice which gives a quantitative description of the experimental scanning data.

In this paper, we present a systematic study of hysteresis and scanning in a simple linear array of slit-shaped graphitic mesopores, composed of two cavities and three necks. The adsorption and desorption of argon at 87K in this model has recently been simulated¹⁷. Our specific aim in this paper is to dissect the associated scanning behaviour in order to reveal the underlying physical mechanism of descending and ascending curves, and to propose a classification for the various types of scanning curve.

2 The model pore network

Figure 2 illustrates our model of a linear array of slit-shaped mesopores, composed of two cavities and three necks, one of which connects the cavities and the other two connect each cavity to the surrounding gas phase. Details of the geometrical parameters can be found in our earlier papers^{17,27}.

3. Discussion

3.1 Scanning in Open end pores, Closed end pores and Closed pores

Adsorption-desorption in three uniform pores provide a reference for subsequent discussion of the linear array of mesopores:

- (a) A pore with two ends open to the surrounding gas.
- (b) A pore with one end closed.
- (c) A pore with two ends closed.

In what follows these will be denoted as O-pore, C1-pore and C2-pore, respectively. In a real material, the C2-pore might represent mesopores with very narrow necks connected to the surrounding. Figure 3 shows the pore models and their respective isotherms for 3, 4, 5 and 6nm pores.

A number of features may be noted from Fig 3:

1. Condensation in the O-pore occurs at a higher pressure than that for the C1-pore of the same width. This is because more adsorbed layers are required in the O-pore before the gas-like core is small enough to induce condensation. However, a meniscus, demarcating the adsorbed film and the gas phase develops in the C1-pore, at the closed end and once it is developed condensation occurs.
2. For a given pore size, the evaporation from the O-pore occurs at a higher pressure than that from the C1-pore because (a) the adsorbate is more cohesive in the C1-pore because of the stronger adsorption field at the closed end and (b) because there is only one end from which evaporation can occur.
3. The condensation pressure is lowest in the C2-pore because there is a meniscus at each end but there is only one in the C1-pore. Evaporation of the condensate from a filled C2-pore is delayed because there is no interface separating the adsorbate and the surrounding gas, and therefore evaporation occurs by stretching the adsorbate until it loses its mechanical stability. In small cavities the cavitation pressure is reduced because of the stabilization of the condensate by the solid-fluid interaction when this is favourable to packing (compare the 3nm C2-pore with larger pores).
4. The adsorption boundary for all pores shifts to higher pressure as the pore width is increased. This is because more adsorbed layers are needed in larger pores before the core is small enough to induce condensation.
5. The desorption boundary for the O-pore and the C1-pore shifts to higher pressure with pore width, due to the larger radius of curvature of the cylindrical interface.

In the linear array of mesopores with two cavities and three necks, four types of scanning behaviour can be observed, which will be discussed in detail in Section 3.6. The physics of the scanning behaviour can be elaborated with the adsorption and desorption mechanisms of above three uniform pores; we have selected one pore configuration in each group for this purpose.

3.2 Group 1

The pore configurations for Group 1 have the following properties: the three necks are equal in size, or two of them have the same width and the third one is smaller. In this group, the descending scanning curve from a partially filled pore with the small cavity full of condensate and the large cavity empty spans the boundary hysteresis loop. The selected example for this group is the pore configuration #1 with three necks smaller than the critical width (H_c). This is the simplest case of connectivity, and therefore the adsorption-desorption isotherm and its scanning curve are rather straightforward. Without loss of generality, we take the case where the three necks are equal in size. The isotherm and a descending scanning curve (*DSC*) are shown in Figure 4 and the schematics of the 2D-density distribution of adsorbate at various points along the adsorption and desorption branches are shown in Figure 5.

Although the main emphasis is on scanning curves, we discuss briefly the mechanisms of adsorption and desorption to facilitate our subsequent discussion on the scanning curve. Adsorption into an empty array begins with molecular layering on the pore walls of the cavities and necks. Condensation occurs first in the necks (Point A) as in the O-pore, because the necks are equivalent to an O-pore prior to condensation. Once the necks have filled with adsorbate, the two cavities become in effect two independent C2-pores, i.e. more layers build up on the pore walls until the gas-like core is small enough to induce condensation. This occurs first in the small cavity at Point B, followed by the larger cavity at Point C. On desorption from a completely filled array, the adsorbate in the cavities are stretched up to Point D, where a first order evaporation occurs via the cavitation mechanism to Point E, after which the necks behave as an O-pore. Therefore, the evaporation from the necks occurs at the same pressure as in the corresponding O-pore of the same size. The vertical evaporation from the two cavities at the same pressures depends on the spatial arrangement of the necks; there are two possibilities for this to occur: either the two large necks are of same size, or the largest neck joins the two cavities in the middle, which corresponds to Groups 1 and 2, respectively. Clearly, the adsorption-desorption isotherm alone cannot discriminate between these two pore configurations. A possible solution is to investigate the scanning curves.

For this Group 1, there is only one possible descending scanning from a partially filled pore where the small cavity is filled with adsorbate and the large cavity is empty, except, of course, for an adsorbed film on the pore walls; this is the segment $B-B'$ in Figure 4. On reducing the pressure from any point along this segment, the descending curve spans the hysteresis loop and meets the vertical desorption boundary at Point F as the condensate stretches in the small cavity the adsorbed layers are thinned in the large cavity. Once this descending curve meets the vertical desorption boundary of the hysteresis loop, evaporation occurs from the small cavity.

The descending scanning curve separates the hysteresis loop into two regions (Figure 4): the blue region above the “horizontal” descending curve is associated with the capacity of the large cavity while the red region underneath the curve is associated with the capacity of the small cavity and the large necks (if they are larger than H_c). This means that when “horizontal” scanning curves are observed in practice the capacity between two consecutive curves corresponds to the size of the cavity associated to the condensation pressure between these two descending curves.

The scanning curve is reversible in the sense that if we stop at any point along this curve and reverse the pressure we would trace the same curve, i.e. there is no sub-loop. This is confirmed by our recent Monte Carlo simulation¹⁷.

3.3 Group 2

The common feature for all the pore configurations of Group 2 is that the neck joining the two cavities is the largest one. The descending scanning curve partially spans the hysteresis loop and returns to the same (adsorption) boundary at a pressure greater than the lower closure point. To illustrate the behaviour of this group, we select the configuration #2.1 with two necks smaller than H_c and the third neck, larger than the H_c , connecting the two cavities. The isotherms and the scanning curves for this configuration are shown in Figure 6 and the 2D-density distributions for various points on the isotherms are shown in Figure 7.

There is a sequence of four condensation steps in adsorption: (1) the two small necks (Point A), (2) the large neck (Point B), (3) the small cavity (Point C) and (4) the large cavity (Point D). On desorption from a completely filled array there is a first order transition from the two cavities by cavitation (Point E to F).

Although the hysteresis loop in Group 2 is similar to Group 1 in that the condensate in the two cavities evaporates at the same pressure, the *DSC* of Group 2 is distinct from Group 1, which could be used as a possible criterion to distinguish between these two groups. The *DSC* for this pore configuration can begin at any point along the two segments *C-C'* and *B-B'*. When the descending scan begins from the segment *C-C'*, where the small cavity is filled with adsorbate, and the large cavity is empty, it spans the interior of the hysteresis loop. Desorption proceeds mainly by the meniscus receding from the large neck joining the two cavities (behaving like a C1-pore), but there is also loss of adsorbate due to stretching of the condensate in the small cavity. When the meniscus reaches the junction between this neck and the small cavity (Point G) the condensate evaporates instantly from in the small cavity at Point H (pore blocking mechanism). The pressure here is greater than the cavitation pressure encountered in desorption from a completely filled array (Points E-F) and therefore the *DSC* from Point C does not join the lower closure point would be commonly observed in experimental scanning curves. This happens because of the wide distribution of cavity and neck widths in real porous solids. As for Group 1, the shaded region between the *DSC* and the adsorption boundary represents the capacity of the small cavity and the large neck.

The other path for a descending scan is from any point along the segment *B-B'*, where all the necks are filled with adsorbate and the two cavities are empty, except for adsorbed layers on the walls. When the scan begins from *B-B'*, the large neck joining the two cavities behaves like an O-pore; therefore the *DSC* scans the hysteresis loop and then returns to the adsorption boundary at Point I, which is very close to Point H. The process is simply evaporation from the large neck.

3.4 Group 3

Group 3 is characterized by having the largest neck connecting the large cavity to the gas surroundings. We selected the pore configuration #2.3 as an example, in which the other two necks are smaller than the critical width H_c . The isotherm and scanning curves are shown in Figure 8 and the 2D-density distributions are shown in Figure 9. The adsorption mechanism

of this linear array is similar that in Group 2. On desorption, the condensate in the large cavity is emptied via the pore blocking mechanism (Point E to F) because the large cavity is connected to the gas surroundings by the largest neck with a width greater than H_c . As pressure is reduced further, the condensate in the small cavity is stretched until it loses mechanical stability and evaporates at the cavitation pressure. Thus the desorption boundary exhibits two steps in the evaporation.

The *DSC* from any point along the segment *C-C'*, where the small cavity is filled with adsorbate and the large cavity remains empty, reveals interesting behaviour, which has not been seen in the last two groups. The *DSC* spans the hysteresis loop to Point H, due to the stretching of the condensate in the small cavity but mainly due to the two receding menisci in the largest neck (behaving like an O-pore). At Point H there is evaporation from the largest neck at a pressure which is slightly greater than the first evaporation from a completely filled pore, in which the largest neck behaves like a C1-pore.

The *DSC* from any point along the *B-B'* segment (where all necks are full and the two cavities are empty) is the same as that discussed for Group 2, which is associated with the evaporation from the largest neck.

The ascending scanning can start at any point along the segment *F-F'* where the two small necks and the small cavity are filled with adsorbate and the largest neck (behaving like an O-pore) and the large cavity are empty. The ascending scanning curve (*ASC*) spans the hysteresis loop, corresponding to molecular layering on the largest neck, followed by condensation at the condensation pressure of this O-pore like largest neck. This pressure is the same as the pressure of Point B. What is interesting is that the *DSC* from *C-C'* segment and the *ASC* from *F-F'* segment form a sub-loop within the hysteresis loop. The sub-loop occurs over the same pressure range as the *DSC* from the *B-B'* segment, and both describe condensation and evaporation in the O-pore like largest neck.

3.5 Group 4

In this group, the configuration has the largest neck connecting the small cavity to the gas surroundings. The ascending and descending curves partially span the hysteresis loop and return to the desorption or adsorption boundaries, respectively. We selected the pore configuration #2.2, for which the remaining two necks are smaller than the critical width H_c . The isotherm and snapshots are shown in Figures 10 and 11, respectively.

The adsorption mechanism in this pore is similar to that for Groups 2 and 3, while the desorption in this group has two evaporation steps as for Group 3, but with a different sequence of evaporation steps. The condensate in the small cavity evaporates first by a pore blocking mechanism (Point F) because it connects to the gas surroundings via the largest neck, followed by the evaporation from the large cavity via cavitation (Point G). This sequence of evaporation distinguishes this group different from the other three groups.

As in Group 2, the *DSC* from any point on the segment $C-C'$, where the necks and the small cavity are filled with adsorbate and the large cavity is empty, scans the hysteresis loop and is associated with the stretching of the condensate in the small cavity and the receding meniscus in the largest neck this being the dominating process. Once this meniscus has reached the junction between the largest neck and the small cavity evaporation occurs by the pore blocking mechanism. The evaporation pressure here is the same as the pressure of the first evaporation from a completely filled pore because in both situations the largest neck behaves like a C1-pore.

The ascending scan can start from any points on the segment $F-F'$ where only the large cavity and the two smaller necks are filled with adsorbate. The *ASC*, which is due to molecular layering in the largest neck and the small cavity, spans the hysteresis loop. This is followed, first by the condensation in the largest neck, which resembles an O-pore (Point J), and then by the condensation in the small cavity at a higher pressure (Point K). It is interesting to note that this ascending scanning curve starts from a point where the large cavity has been filled with adsorbate, and the scan is associated with the condensation in the largest neck and then in the small cavity. This is in contrast to adsorption in an empty pore where condensation in the small cavity occurs first, and is then followed by condensation in the large cavity. It is also interesting to note that the sub loops formed in the *ASC* and the *DSC* are related to the small cavity and the largest neck (shaded region).

Descending scanning from any point along the segment $J-J'$, where the small cavity and the large neck are filled, partially spans the hysteresis loop and returns to the ASC from Point F, which is attributed to the evaporation from the large neck behaving like an O-pore. This forms a sub-loop within the main hysteresis loop. It is clear that the sub-loop is associated with the condensation and evaporation of the large neck.

3.6 Classification of pore configurations based on scanning curves

In a linear array of mesopores with two cavities and three necks, there are 26 different ways of arranging the cavities and necks, with respect to their size, and whether the necks are smaller or larger than the critical pore width, H_c , which distinguish two modes of evaporation in the cavity: cavitation and pore blocking, respectively. The schematics of the isotherms and their scanning curves for these 26 pore configurations are presented in Table 1.

We classify the associated scanning curves into the following four groups illustrated in Table 2, each with identifiable characteristics:

1. Group 1:
 - a. Evaporation from both cavities is a first order phase transition and occurs at the same pressure, which is either equal to the cavitation pressure (cavitation) or greater than the cavitation pressure (pore blocking).
 - b. The small cavity is filled with condensate and the large cavity is empty, except for an adsorbed film on its pore walls. Descending curves from a partially filled array span the hysteresis loop and meet the vertical boundary of the desorption branch.
2. Group 2:
 - a. Evaporation is the same as described for Group 1.
 - b. The descending curve partially spans the hysteresis loop and then falls vertically onto the same (adsorption) boundary instead of onto the vertical desorption boundary of the hysteresis loop as in Group 1.
3. Group 3:

- a. Evaporation occurs in two stages: a first order evaporation from the large cavity followed by a second first order evaporation from the small cavity
 - b. The descending scanning curve spans the hysteresis loop and meets the junction between the two evaporation steps.
 - c. There is a small sub-loop associated with the filling and emptying of the large neck.
4. Group 4: This group has more complex characteristics than the other groups:
- a. Evaporation also occurs in two stages as in Group 3, but in this case, the small cavity is emptied first, followed by the large cavity at a lower pressure.
 - b. The descending curve from a partially filled array, in which the small cavity is filled with adsorbate and the large cavity is empty, is similar to that in Group 2; partially spanning the hysteresis loop and then falling vertically onto the adsorption boundary of the hysteresis loop when the condensate evaporates from the small cavity.
 - c. The ascending curve from a partially filled array, with the large cavity filled with adsorbate and the small cavity empty, partially spans the hysteresis loop and falls with increasing gradient onto the desorption boundary as condensate occurs in the small cavity.

4. Conclusions

We have carried out an extensive study of adsorption-desorption and scanning in a linear array of mesopores consisting of two cavities and three necks. Depending on the relative size of the cavities and necks and their connectivity, there are 26 combinations of pore arrays, which can be categorized into four groups according to the character of their scanning curves:

- (i) Group 1: the *DSC* spans the hysteresis loop and meets the vertical desorption boundary of the hysteresis loop. This is due to stretching of the adsorbate in the small cavity; it separates the loop into two regions which are associated with the capacities of the large and small cavities,
- (ii) Group 2: the *DSC* partially spans the loop and returns to the adsorption boundary which is due to either evaporation from the small cavity via pore blocking or from the large neck,
- (iii) Group 3: the *DSC* spans across the loop and meets the junction between the two evaporation steps by a mechanism similar to Group 1, but there is a sub-loop which is associated with the filling and emptying of the large neck,
- (iv) Group 4: the *DSC* behaves like that in Group 2 while the *ASC* from the configuration, where the large cavity is full of adsorbate and the small cavity is empty, partially spans the loop and returns to the desorption boundary, due to the condensation in the small cavity. The sub-loop is once again due to the filling and emptying of the largest neck.

Reference

1. Thommes, M. Physical Adsorption Characterization of Ordered and Amorphous Mesoporous Materials. In *Nanoporous Materials, Science & Engineering Volume 4*. Edited by Lu G, Zhao XS. New Jersey: Imperial College Press; **2004**, 317-364
2. Everett, D. H.;Haynes, J. M. Capillarity and Porous Materials: Equilibrium Properties. *Colloid Science*. **1973**, 123-172.
3. Horikawa, T.; Do, D. D.;Nicholson, D. Capillary Condensation of Adsorbates in Porous Materials. *Adv Colloid Interfac*. **2011**, *169*, 40-58.
4. De Boer, J. H. The Structure and Texture of a Physical Adsorbent. *Colloques Internationaux du CNRS*. **1972**, *201*, 407.
5. Sing, K. S. W.; Everett, D. H.; Haul, R. A. W.; Moscou, L.; Pierotti, R. A.; Rouquerol, J.;Siemieniewska, T. Reporting Physisorption Data for Gas/Solid Systems with Special Reference to the Determination of Surface Area and Porosity (Recommendations 1984). *Pure Appl Chem*. **1985**, *57*, 603-619.
6. Sing, K. S. W.;Williams, R. T. Physisorption Hysteresis Loops and the Characterization of Nanoporous Materials. *Adsorpt Sci Technol*. **2004**, *22*, 773-782.
7. McBain, J. W. An Explanation of Hysteresis in the Hydration and Dehydration of Gels. *J Am Chem Soc*. **1935**, *57*, 699-700.
8. Rasmussen, C. J.; Vishnyakov, A.; Thommes, M.; Smarsly, B. M.; Kleitz, F.;Neimark, A. V. Cavitation in Metastable Liquid Nitrogen Confined to Nanoscale Pores. *Langmuir*. **2010**, *26*, 10147-10157.
9. Ravikovitch, P. I.;Neimark, A. V. Density Functional Theory of Adsorption in Spherical Cavities and Pore Size Characterization of Templated Nanoporous Silicas with Cubic and Three-Dimensional Hexagonal Structures. *Langmuir*. **2002**, *18*, 1550-1560.
10. Neimark, A. V.;Vishnyakov, A. The Birth of a Bubble: A Molecular Simulation Study. *J Chem Phys*. **2005**, *122*, 054707-1-054707-10.
11. Esparza, J. M.; Ojeda, M. L.; Campero, A.; Hernández, G.; Felipe, C.; Asomoza, M.; Cordero, S.; Kornhauser, I.;Rojas, F. Development and Sorption Characterization of Some Model Mesoporous and Microporous Silica Adsorbents. *J Mol Catal A-chem*. **2005**, *228*, 97-110.
12. Morishige, K. Effects of Carbon Coating and Pore Corrugation on Capillary Condensation of Nitrogen in Sba-15 Mesoporous Silica. *Langmuir*. **2013**, *29*, 11915-11923.
13. Morishige, K. Hysteresis Critical Point of Nitrogen in Porous Glass: Occurrence of Sample Spanning Transition in Capillary Condensation. *Langmuir*. **2009**, *25*, 6221-6226.
14. Tompsett, G. A.; Krogh, L.; Griffin, D. W.;Conner, W. C. Hysteresis and Scanning Behavior of Mesoporous Molecular Sieves. *Langmuir*. **2005**, *21*, 8214-8225.
15. Klomkliang, N.; Do, D. D.;Nicholson, D. Effects of Temperature, Pore Dimensions and Adsorbate on the Transition from Pore Blocking to Cavitation in an Ink-Bottle Pore. *Chem Eng J*. **2014**, *239*, 274-283.
16. Klomkliang, N.; Do, D. D.;Nicholson, D. Hysteresis Loop and Scanning Curves of Argon Adsorption in Closed-End Wedge Pores. *Langmuir*. **2014**, *30*, 12879-12887.
17. Klomkliang, N.; Do, D. D.;Nicholson, D. Hysteresis Loop and Scanning Curves for Argon Adsorbed in Mesopore Arrays Composed of Two Cavities and Three Necks. *J Phys Chem C*. **2015**, *119*, 9355-9363.
18. Ball, P. C.;Evans, R. Temperature Dependence of Gas Adsorption on a Mesoporous Solid: Capillary Criticality and Hysteresis. *Langmuir*. **1989**, *5*, 714-723.
19. Puibasset, J. Monte-Carlo Multiscale Simulation Study of Argon Adsorption/Desorption Hysteresis in Mesoporous Heterogeneous Tubular Pores Like Mcm-41 or Oxidized Porous Silicon. *Langmuir*. **2009**, *25*, 903-911.
20. Hitchcock, I.; Lunel, M.; Bakalis, S.; Fletcher, R. S.; Holt, E. M.;Rigby, S. P. Improving Sensitivity and Accuracy of Pore Structural Characterisation Using Scanning Curves in Integrated Gas Sorption and Mercury Porosimetry Experiments. *J Colloid Interf Sci*. **2014**, *417*, 88-99.

21. Everett, D. H.; Smith, F. W. A General Approach to Hysteresis II Development of the Domain Theory. *Trans Faraday Soc.* **1954**, *50*, 187-197.
22. Broekhoff, J. C. P.; van Beek, W. P. Scanning Studies on Capillary Condensation and Evaporation of Nitrogen. Part 2.-Analysis of Ascending and Descending Scanning Curves within B-Type Hysteresis Loops. *J Chem Soc Farad T 1.* **1979**, *75*, 42-55.
23. Coasne, B.; Gubbins, K. E.; Pellenq, R. J. M. Domain Theory for Capillary Condensation Hysteresis. *Phys Rev B.* **2005**, *72*, 024304-9.
24. Mason, G. Determination of the Pore-Size Distributions and Pore-Space Interconnectivity of Vycor Porous Glass from Adsorption-Desorption Hysteresis Capillary Condensation Isotherms. *P R Soc Lond A Mat.* **1988**, *415*, 453-486.
25. Rojas, F.; Kornhauser, I.; Felipe, C.; Esparza, J. M.; Cordero, S.; Dominguez, A.; Riccardo, J. L. Capillary Condensation in Heterogeneous Mesoporous Networks Consisting of Variable Connectivity and Pore-Size Correlation. *Phys Chem Chem Phys.* **2002**, *4*, 2346-2355.
26. Cimino, R.; Cychosz, K. A.; Thommes, M.; Neimark, A. V. Experimental and Theoretical Studies of Scanning Adsorption-Desorption Isotherms. *Colloid Surface A.* **2013**, *437*, 76-89.
27. Nguyen, P. T. M.; Fan, C.; Do, D. D.; Nicholson, D. On the Cavitation-Like Pore Blocking in Ink-Bottle Pore: Evolution of Hysteresis Loop with Neck Size. *J Phys Chem C.* **2013**, *117*, 5475-5484.

Figure Captions

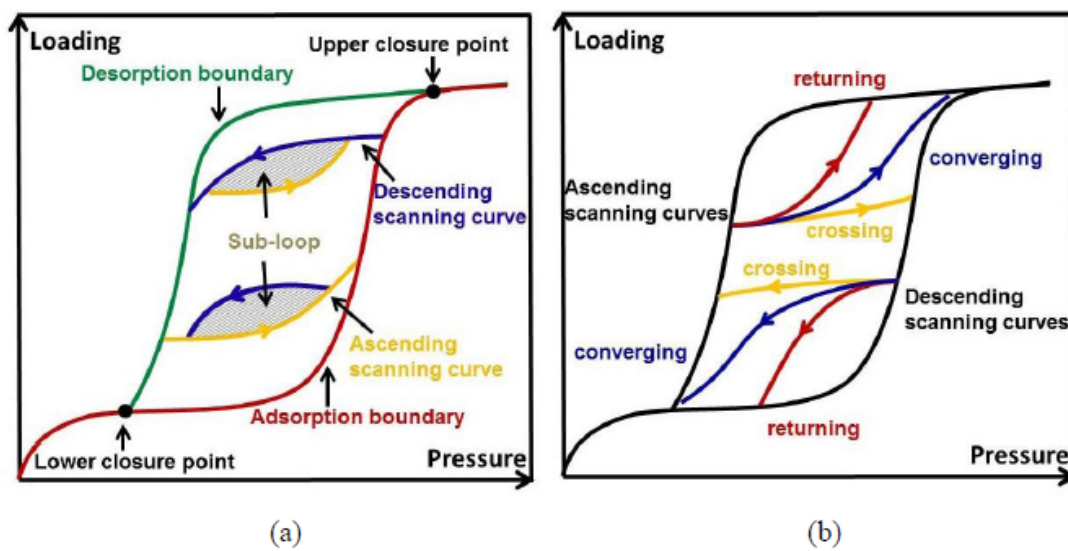


Figure 1. Schematic diagram of (a) adsorption-desorption isotherm with scanning curves; (b) three different types of scanning curves.

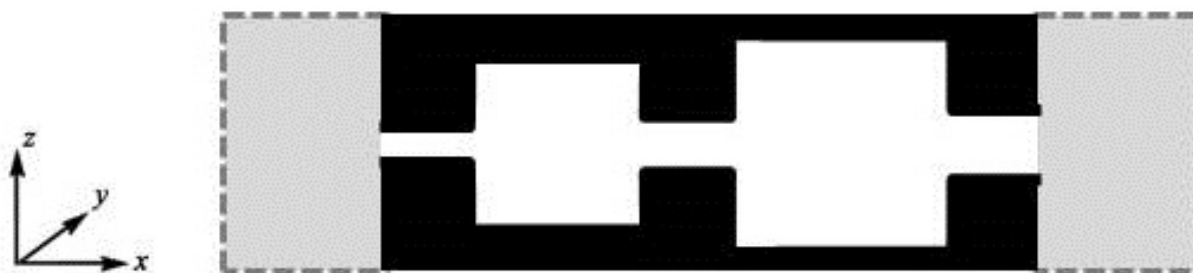


Figure 2. Schematic diagram of the model of linear array of slit mesopores. The dark region indicates the solid phase and grey region shows the bulk gas phase.

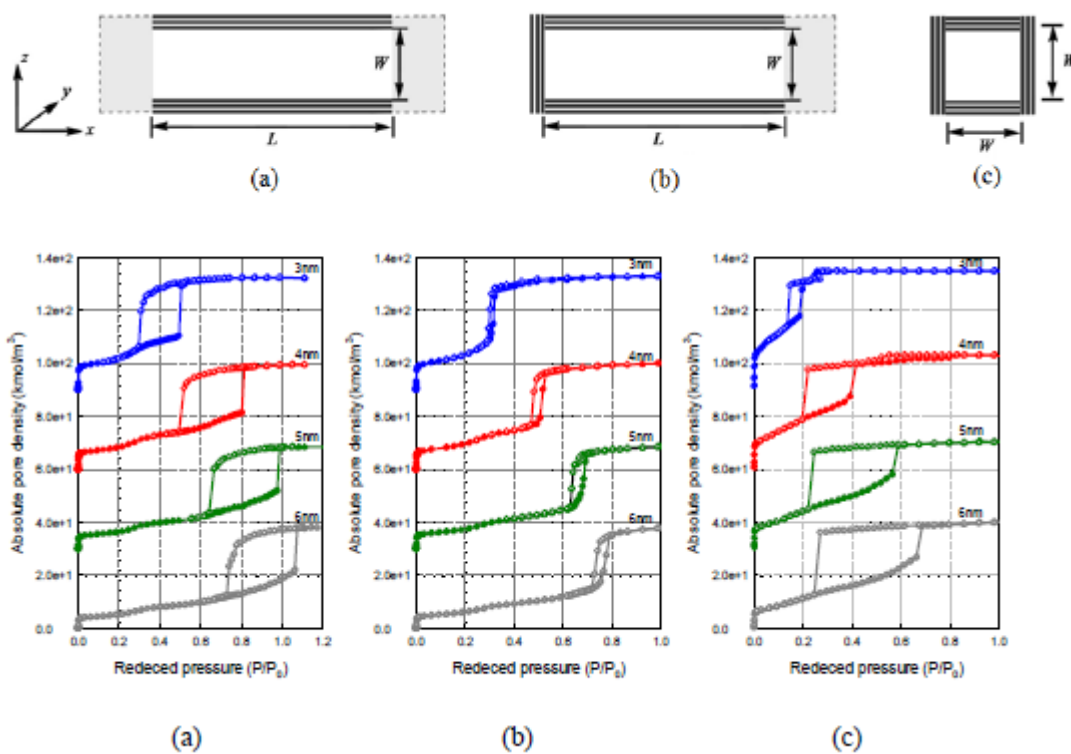


Figure 3. Top panel: Schematic diagrams of three uniform pore models. Bottom panel: Simulated isotherms for argon at 87K in uniform pores with different widths: (a) open end pores of length 20nm, (b) closed end pores of length 20nm and (c) closed pores with lengths the same as their width.

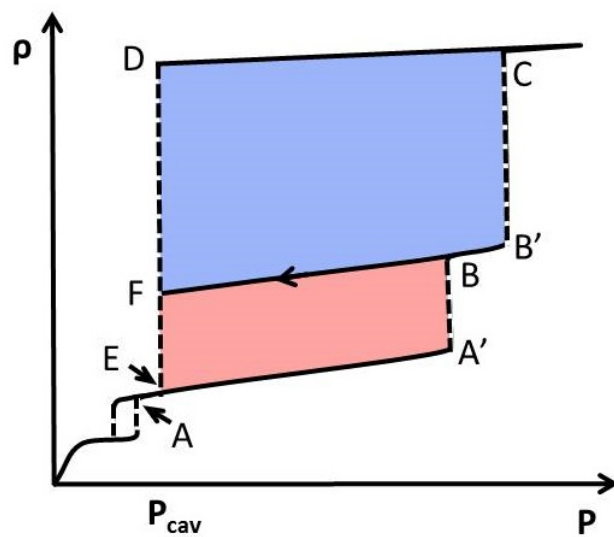


Figure 4: Adsorption and desorption isotherms and scanning curves for pore configuration #1. Dashed lines indicate the irreversible phase transition (condensation and evaporation).

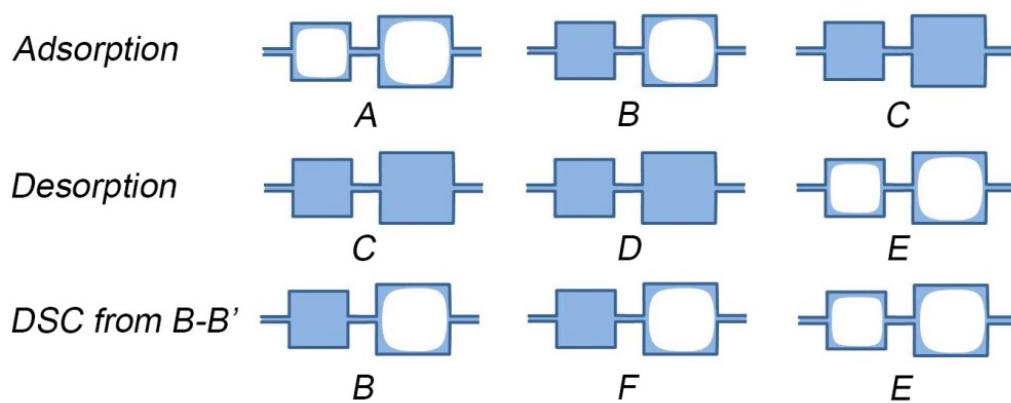


Figure 5. Schematic of the adsorbate in pore configuration #1. The labels correspond to those in Figure 4.

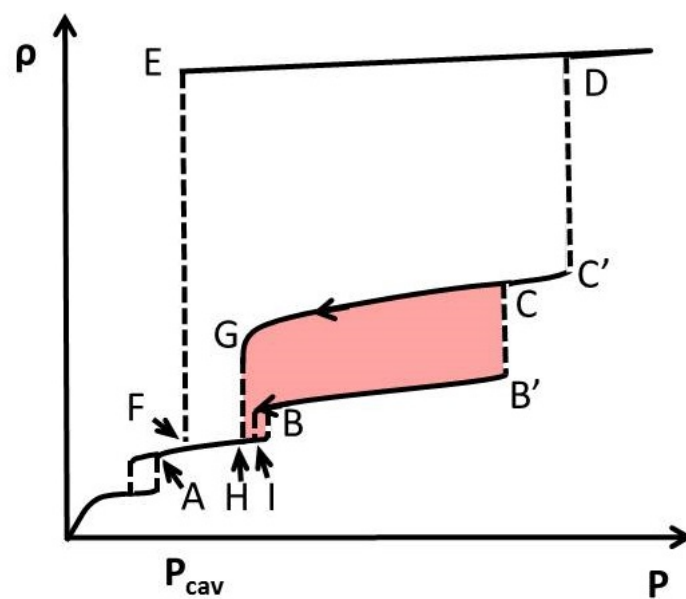


Figure 6: Adsorption-desorption isotherms and scanning curves for pore configuration #2.1. Dashed lines indicate the irreversible phase transition (condensation and evaporation). The shaded region indicates the capacity of the small cavity.

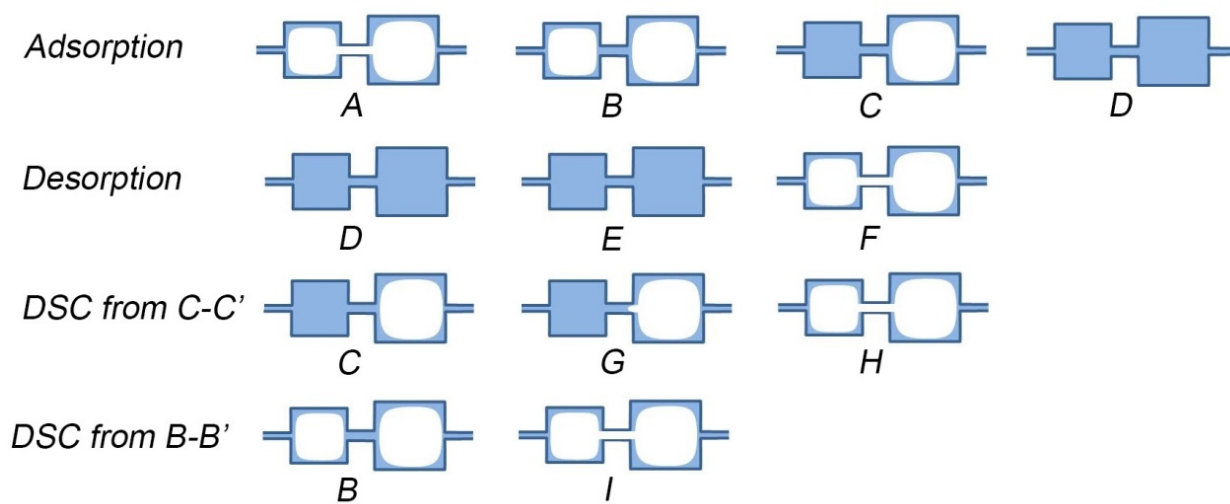


Figure 7. Schematic of the adsorbate in pore configuration #2.1. The labels correspond to those in Figure 6.

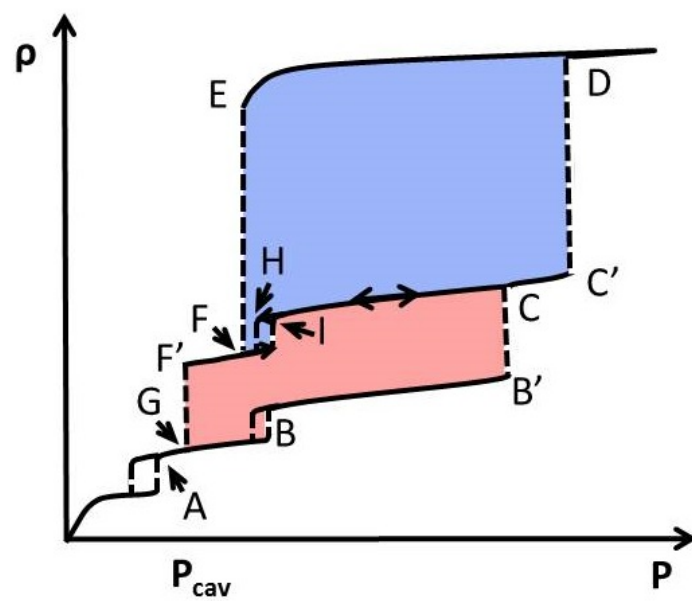


Figure 8: Adsorption-desorption isotherms and scanning curve for pore configuration #2.3. Dashed lines indicate the irreversible phase transition (condensation and evaporation).

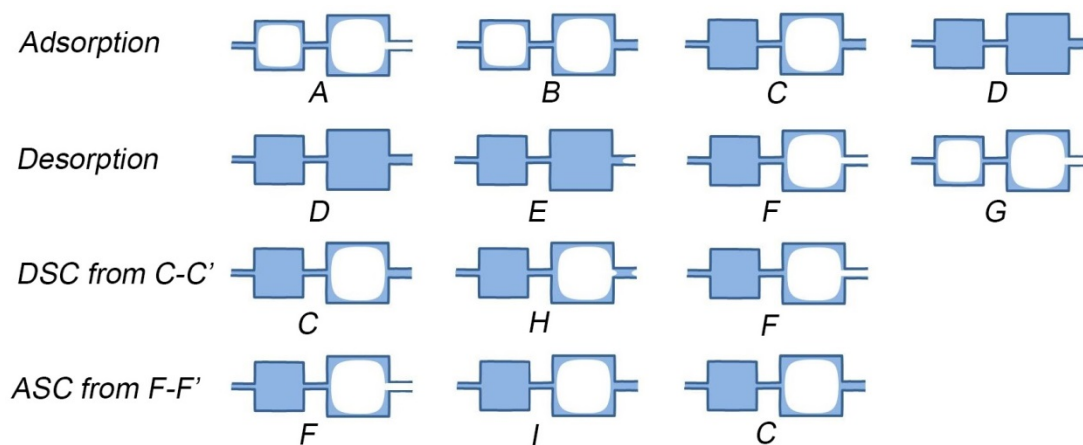


Figure 9. Schematic of the 2D-density distribution of adsorbate in pore configuration #2.3. The labels correspond to those in Figure 8.

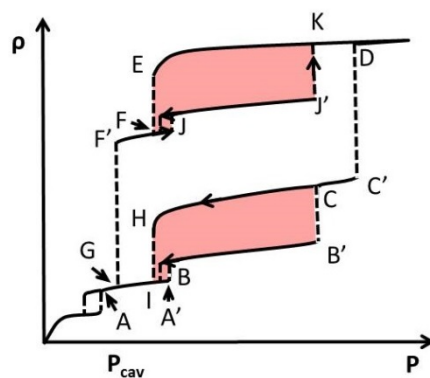


Figure 10: Adsorption-desorption isotherms and scanning curves for pore configuration #2.2. Dashed lines indicate the irreversible phase transition (condensation and evaporation).

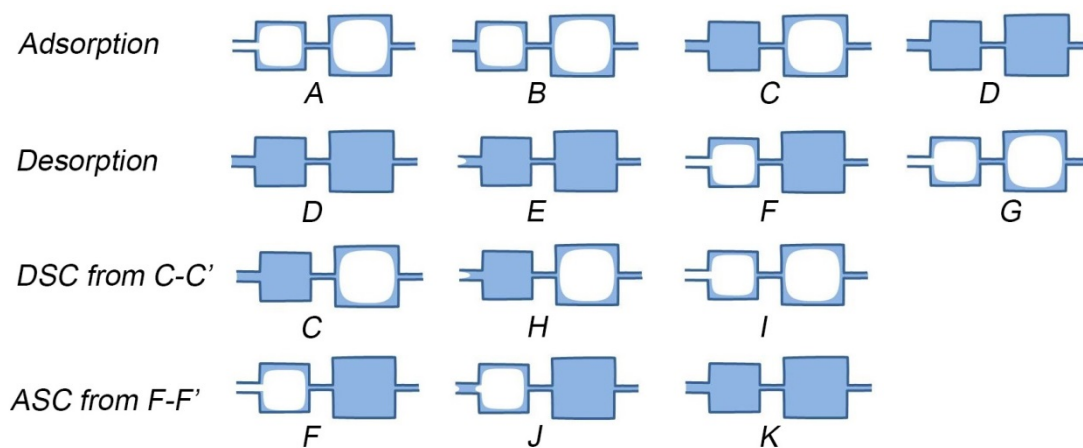
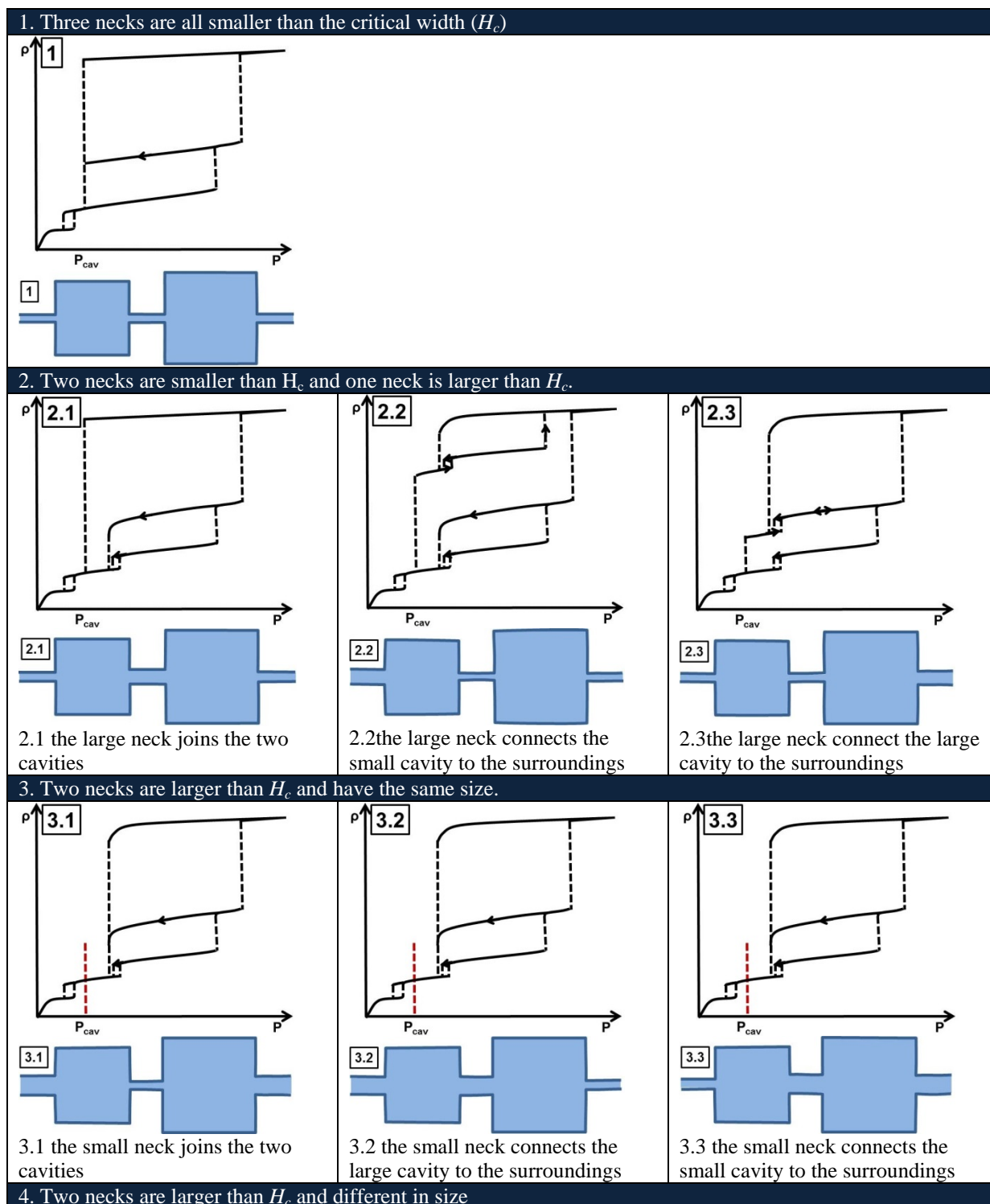
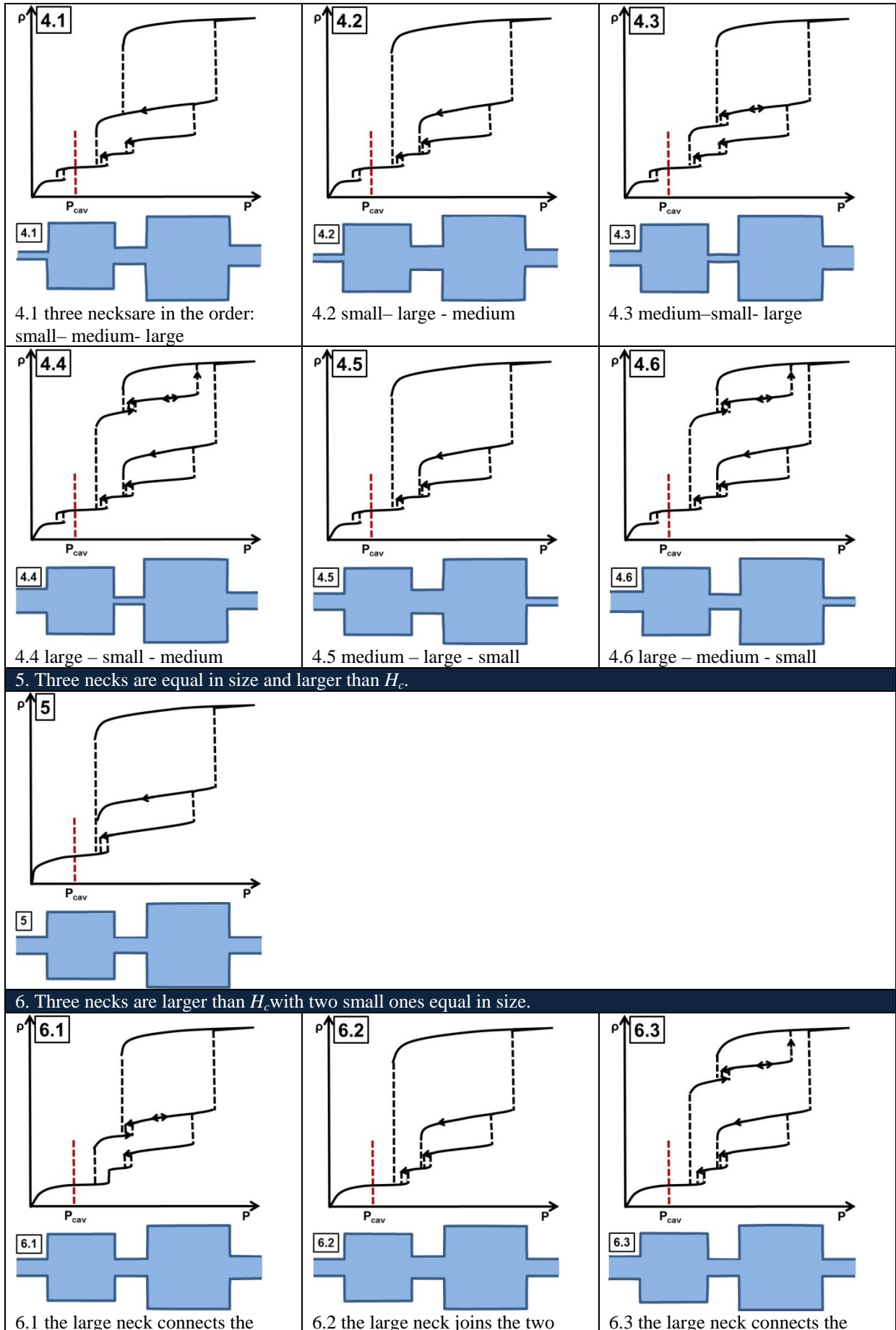


Figure 11. Schematic of the adsorbate in pore configuration #2.2. The labels correspond to those in Figure 10.

Tables

Table 1: Different pore configurations and their adsorption, desorption and scanning behaviours



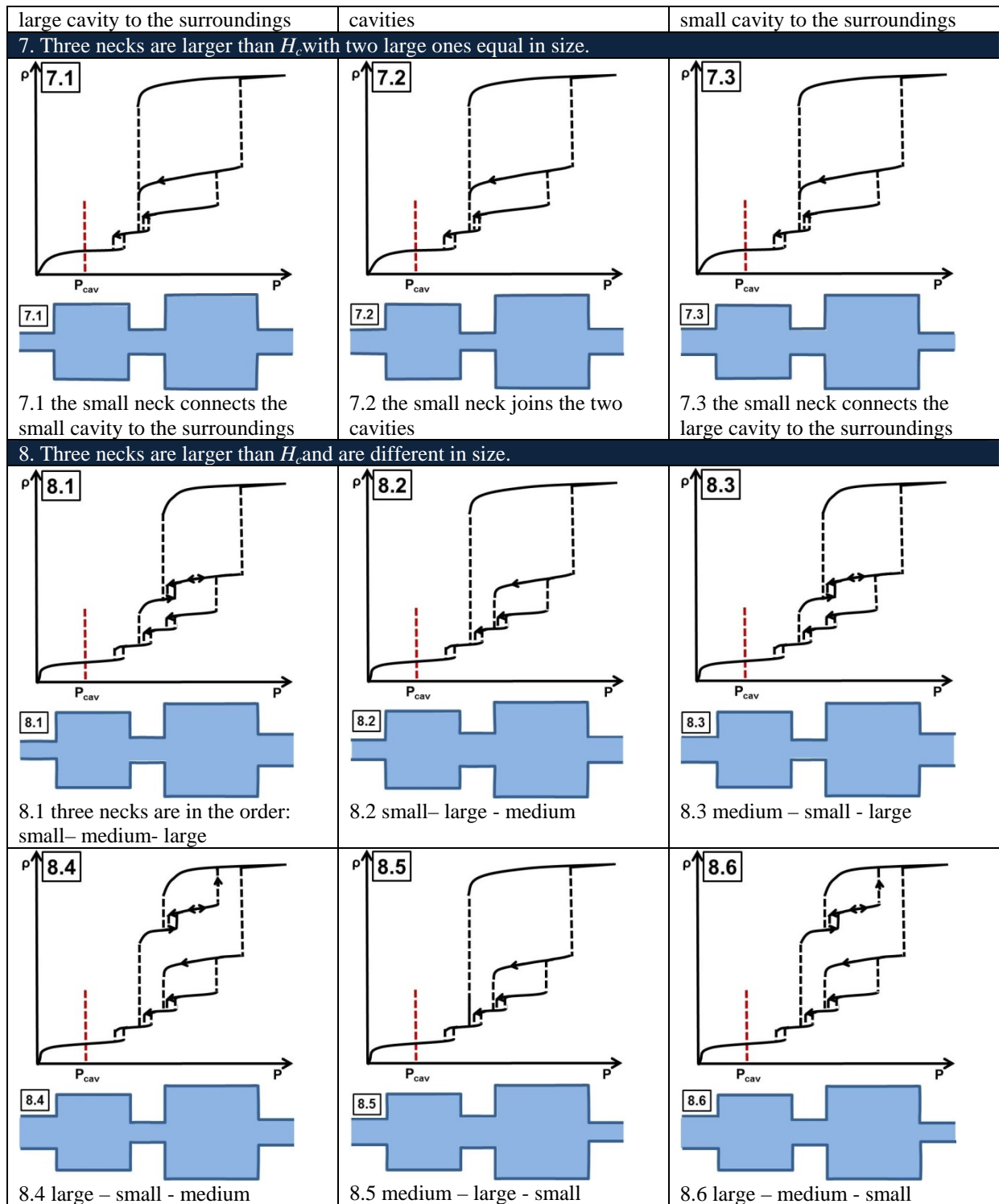


Table 2. Classification of the pore configurations in 4 groups according to the pattern of scanning curves

GROUP 1	
#1, #3.1, #3.2, #3.3, #5, #7.1, #7.2, #7.3	
GROUP 2	
#2.1, #4.2, #4.5, #6.2, #8.2, #8.5	
GROUP 3	
#2.3, #4.1, #4.3, #6.1, #8.1, #8.3	
GROUP 4	
#2.2, #4.4, #4.6, #6.3, #8.4, #8.6	